

Prediction of ambient-pressure superconductivity in ternary hydride PdCuH_x

Cite as: J. Appl. Phys. **131**, 033903 (2022); <https://doi.org/10.1063/5.0076728>

Submitted: 27 October 2021 • Accepted: 02 January 2022 • Published Online: 20 January 2022

 R. Vocaturo,  C. Tresca,  G. Ghiringhelli, et al.

COLLECTIONS

Paper published as part of the special topic on [Phenomena of Hydrides](#)



View Online



Export Citation



CrossMark

ARTICLES YOU MAY BE INTERESTED IN

[Hydrogen in single-crystalline anatase TiO₂](#)

Journal of Applied Physics **131**, 030902 (2022); <https://doi.org/10.1063/5.0076694>

[Growth of bulk β-Ga₂O₃ single crystals by the Czochralski method](#)

Journal of Applied Physics **131**, 031103 (2022); <https://doi.org/10.1063/5.0076962>

[Strain-tunable in-plane ferroelectricity and lateral tunnel junction in monolayer group-IV monochalcogenides](#)

Journal of Applied Physics **131**, 034101 (2022); <https://doi.org/10.1063/5.0072124>



Applied Physics
Reviews

Read. Cite. Publish. Repeat.

19.162
2020 IMPACT FACTOR*

Prediction of ambient-pressure superconductivity in ternary hydride PdCuH_x

Cite as: J. Appl. Phys. **131**, 033903 (2022); doi: 10.1063/5.0076728

Submitted: 27 October 2021 · Accepted: 2 January 2022 ·

Published Online: 20 January 2022



View Online



Export Citation



CrossMark

R. Vocaturo,¹ C. Tresca,^{2,a)} G. Chiringhelli,¹ and G. Profeta^{2,3,a)}

AFFILIATIONS

¹Dipartimento di Fisica Politecnico di Milano, piazza Leonardo da Vinci 32, I-20133 Milano, Italy

²Dipartimento di Scienze Fisiche e Chimiche, Università degli studi dell'Aquila, Via Vetoio 10, I-67100 L'Aquila, Italy

³CNR-SPIN, Via Vetoio 10, I-67100 L'Aquila, Italy

Note: This paper is part of the Special Topic on Phenomena of Hydrides.

a) Authors to whom correspondence should be addressed: cesare.tresca@aquila.infn.it and gianni.profeta@aquila.infn.it

ABSTRACT

We present an *ab initio* study of the ternary hydride PdCuH_x, a parent compound of the superconducting PdH, at different hydrogen content ($x = 1, 2$). We investigate its structural, electronic, dynamical, and superconducting properties, demonstrating that, at low hydrogen content, the system is not a superconductor above 1 K; however, the highly hydrogenated structure is a strongly coupled superconductor. We give a solid rationale for the unusual increase of the superconducting critical temperature in hydrogenated palladium when alloyed with noble metals (Cu, Ag, and Au), as observed in Stritzker's experiments in 1972 [B. Stritzker, Z. Phys. **268**, 261–264 (1974)] but never investigated with modern experimental and theoretical techniques. We highlight the important role played by H-derived phonon modes at intermediate frequencies, dynamically stabilized by anharmonic effects, as they strongly couple with states at the Fermi level. We hope that the present results will stimulate additional experimental investigations of structural, electronic, and superconducting properties of hydrogenated palladium–noble metal alloys. Indeed, if confirmed, these compounds could be considered a novel class of superconducting hydrides, showing different coupling mechanisms, which can be exploited to engineer new ambient-pressure superconductors.

Published under an exclusive license by AIP Publishing. <https://doi.org/10.1063/5.0076728>

I. INTRODUCTION

The discovery of high-temperature superconducting hydrides definitely changed the scenario of the research on superconducting materials, allowing for the first time to observe superconductivity at room-temperature. This achievement is the last piece of a puzzle begun in 1968 when Ashcroft proposed metallic hydrogen as a high-temperature superconductor.¹

His prediction of the superconducting critical temperature (T_C) around 100 K was based on a conventional (electron–phonon driven) mechanism arising from the strong electron–phonon coupling and high-frequency modes provided by hydrogen in its metallic phase.

Unfortunately, the metallization of hydrogen is extremely difficult and challenging, and only recently, the required pressures ($P > 400$ GPa) have been achieved, bringing new experimental evidences on the metallization of solid hydrogen.^{2,3} However, to overcome the experimental challenges of the early attempts,^{4–6} in 2004,

Ashcroft suggested to move the attention to hydrogen-rich compounds: he speculated that a metallic phase could be favored⁷ exploiting the mechanism of *chemical precompression* induced by the hosting matrix. This idea marked the beginning of an extensive theoretical and experimental search,⁸ which still remains an important topic in the field of condensed matter physics. A major role was undoubtedly played by *ab initio* computational approaches to the superconducting phase, which successfully guided the experimental research toward the discovery of high-temperature superconductivity in sulfur hydride⁹ (T_C of 200 K at $P \approx 200$ GPa) and in lanthanum and yttrium hydrides under pressure^{10–14} ($T_C \approx 250$ K at $P = 150–190$ GPa). Unfortunately, most of the known high-pressure superconducting hydrides cannot be stabilized at ambient pressure but rather transform into other phases (mostly insulating ones). Therefore, they always need to be compressed up to millions of atmosphere (hundreds of GPa) to induce a metallic transition, hindering any technological application. In

addition, experimental investigations are very delicate and expensive; therefore, at the moment, they are performed only by a few highly specialized groups in the world.

In view of these difficulties, nowadays, theoretical and experimental efforts are instead focusing on lowering the superconducting transition pressure, rather than on further increasing the critical temperature.¹⁵ To this end, in a recent special issue,¹⁵ the community indicated important experimental and theoretical challenges that need to be addressed. One of the first suggestions proposed to overcome these challenges is to shift the attention from binary systems—such as sulfur (SH₃) and lanthanum (LaH₁₀) hydrides—to ternary ones. Indeed, the interest for these ternary compounds grew exponentially as Dias and co-workers achieved room-temperature superconductivity (with $T_C = 287$ K) in C–S–H at $P \approx 270$ GPa.¹⁶ Although many questions on this result remain unanswered, as the exact determination of the crystal structure of the superconducting phase,¹⁷ this discovery is extremely important demonstrating that ternary superconducting hydrides can also be stabilized,¹⁵ broadening the spectrum of possibilities to search for new promising superconductors, which may also be stable at lower pressure.^{18–24}

Interestingly, the first superconducting hydrides were discovered at ambient pressure: Th₄H₁₅²⁵ and, in particular, palladium hydride (PdH).^{8,26} PdH is a binary compound with $T_C = 8–9$ K,^{26,27} which was deeply studied both in the past and recently^{8,28} with reports of critical temperature as high as 60 K.²⁹ Due to the high hydrogen affinity of pure palladium, the PdH system has always attracted much theoretical and experimental interest with the aim of increasing even further its H-storage capacity.^{30,31}

Remarkably, in 1974, Stritzker reported the growth of ternary hydrides Pd–M–H, where M stands for noble metals, such as copper, silver, or gold,³² with unexpected superconducting behaviors. In Stritzker's experiment, the Pd–noble metal alloys were made by arc-melting in ultrapure Argon, then pre-charged with H₂-gas, and subsequently implanted with H-atoms at He-temperatures. After implantation of 6×10^{17} H-atoms/cm², superconductivity was observed with the highest critical temperature of 17 K, reported for (Pd_{0.55}Cu_{0.45})H_{≈0.7}³² hydride, i.e., for an H:Metal-ratio ≈ 0.7 . The increase of the critical temperature with respect to pure PdH was also reported for Pd–(Ag,Au)–H systems, with maximum T_C of 15.6 and 13.6 K, respectively. Although potentially very important, Stritzker's evidences³² on ternary hydrides were not sufficiently pursued in the past, resulting practically unexplored from both the experimental and theoretical point of view.

With the renewed interest in superconducting hydrides, especially in ternary systems at low pressure, Stritzker's work probably deserves more attention. Indeed, the enormous difference in pressure between these systems and the high- T_C hydrides suggests a different role played by hydrogen, which is now unlikely to form a metallic sub-lattice. This exciting possibility broadens the scenario previously imagined by Ashcroft, opening new frontiers in engineering novel superconductors with promising properties.

To shed light on this class of ambient-pressure superconducting ternary hydrides, in this work, we explore the structural, electronic, dynamical, and superconducting properties of the

palladium-(copper) hydride by means of first-principles density functional theory (DFT) to predict a possible superconducting phase and understand its microscopic origin. We started our work studying the palladium–copper alloy and then predict the most stable sites for the interstitial hydrogen. We obtain electronic and vibrational properties of the structure of interest to finally predict their superconducting properties.

II. COMPUTATIONAL METHODS

We investigated structural, electronic, and vibrational properties by means of DFT calculations through the *Quantum ESPRESSO*^{33,34} package. The local density approximation (LDA)³⁵ has been used for the exchange–correlation potential. Ultrasoft pseudopotentials³⁶ were used for Pd and Cu, with the valence configurations $4d^9 5s^1 5p^0$ and $3s^2 3p^6 3d^8 4s^2 4p^0$, respectively, while a norm conserving pseudopotential was used for hydrogen.³⁷ Self-consistent calculations were carried out with an energy cut-off on the plane wave expansion of 80 Ry (800 Ry on the electron density). For structural optimization and stress tensor minimization, the energy cut-off was enhanced to 120 Ry (and the cut-off on the electron density to 1200 Ry) to ensure energy and pressure convergence. The sampling of the Brillouin zone (BZ) was performed with a uniform $18 \times 18 \times 18$ k -grid mesh for the PdCu cubic cell (see Sec. III) and then consistently scaled for other structures to ensure the same sampling density of the BZ for all electronic calculations.

Phonon calculations were performed using density functional perturbation theory (DFPT)³⁸ within the harmonic approximation, as implemented in *Quantum ESPRESSO*,^{33,34} and sampling the reciprocal space with a $6 \times 6 \times 6$ grid.³⁹ The superconducting critical temperature was estimated using the Allen and Dynes equation for T_C ,⁴⁰

$$T_C = \frac{\omega_{\log}}{1.2} \exp \left[- \frac{1.04(1 + \lambda)}{\lambda - \mu^*(1 + 0.62\lambda)} \right], \quad (1)$$

which requires the e - ph coupling constant λ and the logarithmic average of the phonon frequency ω_{\log} , both obtained from the electron–phonon coupling function $\alpha^2 F(\omega)$.⁸ The μ^* parameter, accounting for the Coulomb repulsion between electrons, was fixed to 0.1, as it has been shown to be a good approximation for a large class of materials. To converge the function $\alpha^2 F(\omega)$, and hence the parameters λ and ω_{\log} , on the tetragonal unit cells (see Sec. III), a grid of $29 \times 29 \times 23$ k -points was chosen to sample the BZ for electronic states. We investigated both the low-stoichiometry structure of the palladium–copper alloy (PdCuH), with H/M = 0.5, and the high-stoichiometry one (PdCuH₂) with H/M = 1, as prototype systems (M refers to the metal content, Pd and Cu).

Graphical representations of the atomic lattices are obtained with the *XCrySDen*⁴¹ software.

III. RESULTS

We first consider the PdCu alloy at equal concentrations of Pd and Cu, stoichiometry very close to Stritzker's samples.³² At this stoichiometry, the system is known to crystallize both in a disordered *fcc*-structure and in an ordered CsCl phase,^{42–45} usually referred as

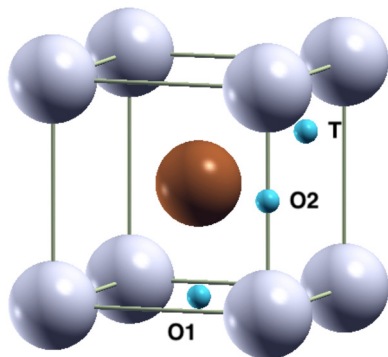


FIG. 1. Unit cell of the PdCu in the CsCl (B2) phase. Gray (brown) spheres represent Pd (Cu) atoms. In the unit cell, the high symmetry intercalation sites of H are indicated with blue points, labeled according to the standard literature on the subject.

the B2-phase (see Fig. 1). Indications on the crystal structure of the superconducting phase, after hydrogen intercalation, can be obtained from dedicated works on the subject.

Hydrogen intercalation was studied by Antonov *et al.*,⁴⁶ who intercalated hydrogen in an ordered *fcc* PdCu and PdAg matrix, finding no superconducting transition above 2 K. Another experimental work by Ruilan *et al.*⁴⁷ suggests that the origin of the superconducting transition lays in the ordering of the crystal; therefore, the *fcc* phase, which spontaneously grows disordered, was discarded as responsible for the superconducting phase. In parallel, Irodova *et al.*⁴⁸ demonstrated that PdAg membranes (which are expected to possess very similar chemical properties with respect to PdCu) tend to self-organize in a B2 sub-lattice after hydrogenation. Finally, a structural phase transition below 770 K from the disordered *fcc* phase to the ordered B2 one was suggested from first-principles calculations.⁴⁹ For all these reasons, we will focus on the B2 phase of the PdCu alloy to search for possible superconducting phases. Total energy calculations predict a cubic unit cell with a lattice constant $a = 2.94 \text{ \AA}$ (in good agreement with experiments^{50,51}). The electronic band structure of this phase, reported in Fig. 2, is characterized by the presence of both Pd and Cu derived *d*-orbitals, in the region from the Fermi level (zero of the energy scale) to -4 eV . Free-electron-like dispersions are evident from about -8 eV and around the Fermi energy. Indeed, the resulting Fermi surface (see the inset in Fig. 2) has essentially a *free-electron*-like shape, with the exception of small pockets around the *M* points in the BZ, having Cu character. The comparison with the band structure of pure palladium⁸ reveals that Cu atoms act as electron dopants, expanding the Fermi surface.

The density of states (DOS) is characterized by three evident peaks around 0.5, 1, and 1.5 eV below the Fermi energy. These peaks originate from dispersion-less flatbands like the one along the $R - M$ and $\Gamma - M$ directions. The Fermi level falls just above a sharp peak in the DOS, suggesting possible electronic instabilities.

We can now move to the study of PdCu-hydrides, first focusing on the lowest H-content system (H/M ratio of 0.5).

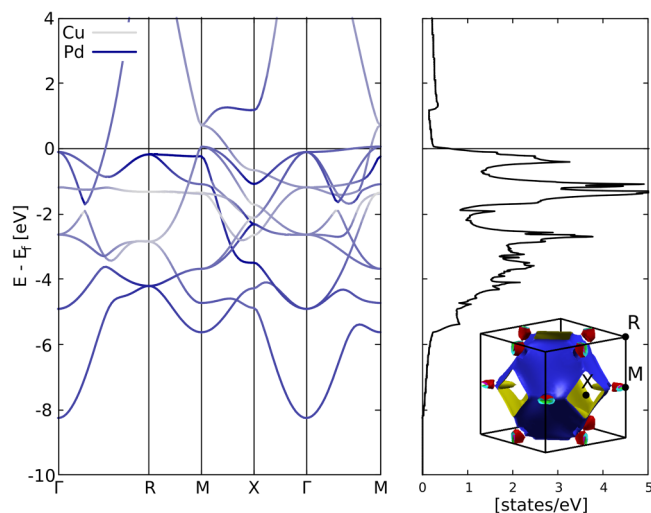


FIG. 2. In the left panel, we report the PdCu projected bands. The Pd (Cu) atomic character of the eigenvalues is plotted in blue (gray). In the right panel, the total density of states is represented. The inset shows the corresponding Fermi surface.

To predict the most stable intercalation site, we performed total energy calculations on a series of randomly placed hydrogen atoms in the PdCu unit cell, followed by relaxation of all the internal degrees of freedom of the system. In Fig. 1, we show the most symmetric absorption sites found after the random search, introducing the common nomenclature: O1 and O2 stand for *octahedral* sites, while T for *tetrahedral*.

The ground-state structure turns out to have H occupying the O1-site (see Fig. 1), resulting in Pd-H layers separated by copper atoms. Due to the loss of cubic symmetry, we find the unit cell expanding in the direction perpendicular to the Pd-H layers, while contracting in the other directions. The final unit cell is, therefore, tetragonal with lattice constants $a = 2.77$ and $c = 3.67 \text{ \AA}$. The occupation of other metastable sites, namely, O2 and T, also leads to tetragonal distortions with total energies higher than the ground state by 160 and 180 meV, respectively. Interestingly, our predicted ground state has a negative formation energy of $\approx -0.3 \text{ eV/cell}$, and its structure is in excellent agreement with neutron diffraction experimental results of Kolshnikov *et al.*⁵² They reported a tetragonal unit cell for the PdCuH_{0.9} system with measured lattice parameters $a = 2.794 \pm 0.005 \text{ \AA}$ and $c = 3.678 \pm 0.008 \text{ \AA}$, which match perfectly our calculations.

The electronic structure of this phase, shown in Fig. 3, highlights that hydrogen is an electron dopant, and it shifts the Fermi level at higher energies with respect to pure PdCu by filling the Pd/Cu derived states. This behavior is in perfect analogy with what has been observed in PdH:⁸ in fact, hydrogen intercalation in pure palladium results in the filling of the former Pd *d*-orbitals, reducing the density of states at the Fermi level.

The Fermi surface of PdCuH is now open: it is composed of two opposite cross-shaped surfaces laying on the *Z* planes and four

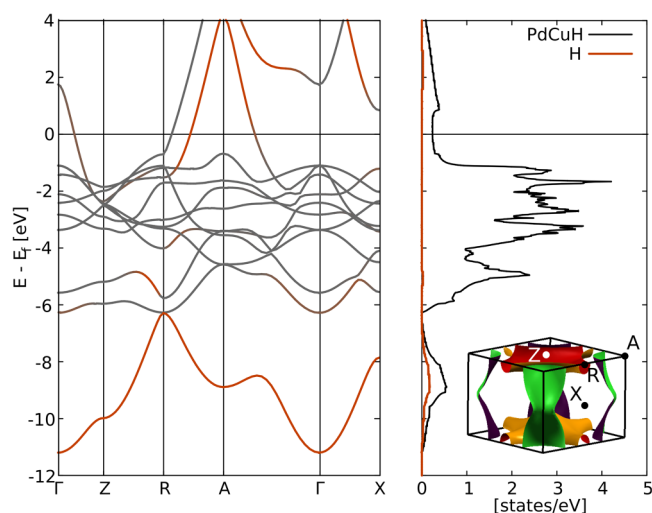


FIG. 3. PdCuH band dispersion (left) and density of states (right). The band presenting a hydrogen-like character is highlighted with a red scale, while the gray scale refers to the metal PdCu character. The black line in the right panel is the total density of states, while the red one refers to the H-projected DOS. The Fermi surface is shown in the inset.

double-cone structures at the corners of the BZ, which extends continuously in the adjacent BZ, parallel to the $\Gamma - Z$ direction.

The stability of the phase was then investigated by calculating phonon dispersion, shown in Fig. 4. The phonon spectrum is characterized by low frequency Pd- and Cu- derived modes and a high frequency region ($\approx 600\text{--}800\text{ cm}^{-1}$) of H-induced modes, separated by a large energy gap. A dynamical instability with a very small negative frequency ($\approx -20\text{ cm}^{-1}$) is observed around the R point of BZ.

However, the presence of this (harmonic) instability was, in part, expected, considering that the same dynamical instability has been reported in PdH.^{53,54} This is representative of a possible non-negligible role of anharmonic effects, whose inclusion can remove the inconsistency, as found for PdH.⁵³

Despite the limitations of the harmonic approximation for this system, the comparison of the calculated phonon density of states with the function $S(Q, \omega)$ reported in Ref. 52 reveals a discrete qualitative agreement with experiments, probably suggesting that anharmonic effects, although surely present, are not as relevant as in PdH.

On the basis of these results, we can predict the superconducting properties of PdCuH,⁵⁵ evaluating the Eliashberg spectral function, $\alpha^2F(\omega)$, reported in Fig. 4.⁵⁶ As shown by the function $\lambda(\omega)$ (see Fig. 4), the coupling is well distributed throughout all the spectrum; however, it results in a predicted total electron-phonon coupling parameter, $\lambda = 0.25$, which gives a $T_C < 1\text{ K}$. We, thus, conclude that, within the present approximations, our results indicate that the PdCuH system is a sub-kelvin superconductor and thus cannot be responsible for the observed T_C in Pd-(noble)metal hydrides. However, the formal concentration reported for the

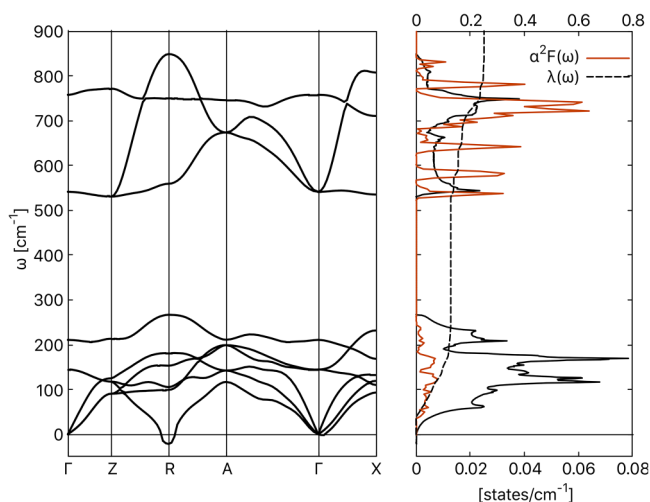


FIG. 4. PdCuH phonon dispersion (right) and relative density of states (left). On the left, we also plot the spectral function (in orange) and its weighted integral $\lambda(\omega)$ (top scale).

superconducting phase is characterized by an H/M ratio of ≈ 0.7 , i.e., a stoichiometry around PdCuH _{≈ 1.4} (see Sec. I), and thus higher than one hydrogen per B2 unit cell. In addition, considering the charging of PdCu with H₂ before H-atom implantation, disorder effects and inhomogeneities can easily stabilize phases with different hydrogen content. For this reason, we extended the study to phases with a higher hydrogen content in the single B2 unit cell, leading to the PdCuH₂ stoichiometry (two hydrogen atoms per B2 unit cell).

The random search for hydrogen intercalation sites in the B2 matrix results in two low energy structures (see Fig. 5) with an energy difference of about $\Delta E \approx 50\text{ meV}$ per unit cell. The ground-state structure has hydrogen occupying both the *octahedral* sites O1 and O2 (see Fig. 1), while the metastable phase is characterized by hydrogen sitting in the *tetrahedral* sites. Interestingly, with the inclusion of vibrational zero-point energy contributions (see below), the octahedral sites turn out to be largely favored with respect to tetrahedral by more than 250 meV.

The inclusion of an additional hydrogen atom in the PdCuH phase results in a very small expansion of the unit cell ($\approx 3\%$ in-plane and $\approx 2.2\%$ out-of-plane), which remains tetragonal, with a negative formation energy of $\approx -0.27\text{ eV/cell}$, demonstrating, once again, the high hydrogen affinity of these compounds. The calculated band structure for the ground state (see Fig. 6) confirms the role of hydrogen as an electron dopant, shifting the Fermi level at higher energies, where the bands now acquire a slightly higher hydrogen character.

The phonon dispersion shows dynamical instabilities around Z and X (see Fig. 7) high symmetry points, with imaginary modes. However, as discussed for PdCuH, anharmonic effects may be crucial for hydrogen-rich compounds and could also (dynamically)

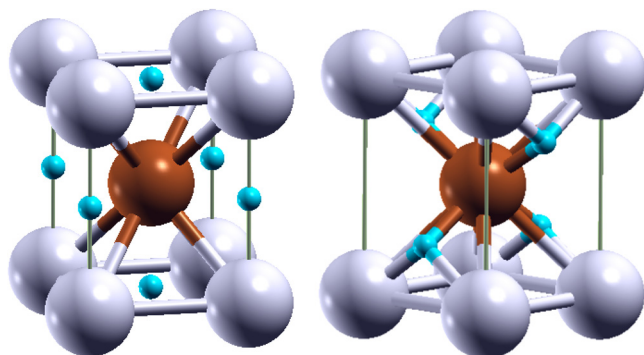


FIG. 5. Ground state (on the left) and metastable (on the right) phases of PdCuH₂.

stabilize the present structure. As reported in Fig. 8, the adiabatic potential energy surface of PdCuH₂ along the normal mode coordinate α , corresponding to the lowest-energy mode at Z, shows weak quartic instability, inducing a small distortion (≈ 0.05 Å), and an energy gain of the order of ≈ 0.5 meV. Due to the very low depth of the double well potential, we can safely speculate that anharmonic effects can stabilize the symmetric, non-distorted, structure, indicating that the equilibrium position of hydrogen atoms is probably dynamical, like in PdH.⁵³

Apart from weak dynamical instabilities, from the phonon dispersion, we observe that PdCuH₂, in contrast with PdCuH, does not present an energy gap at intermediate frequencies, which are the most coupled ones (as observed in palladium hydride⁵³),

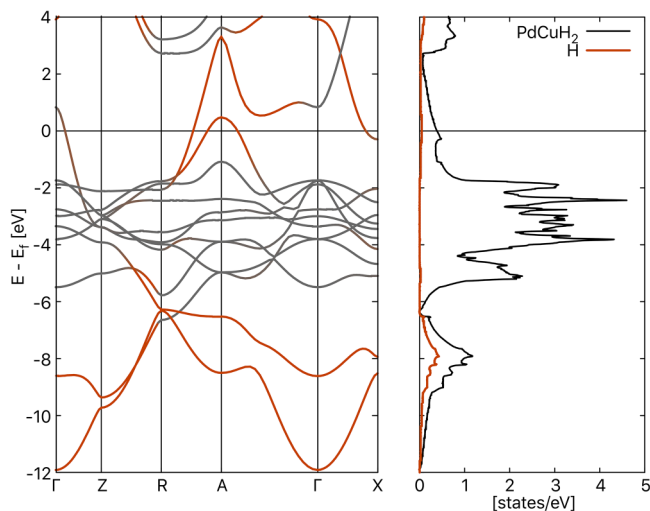


FIG. 6. PdCuH₂ band dispersion (left) and density of states (right). The band presenting a hydrogen-like character is highlighted with a red scale, while the gray scale refers to the metal PdCu character. The black line in the right panel is the total density of states, while the red one refers to the H-projected DOS.

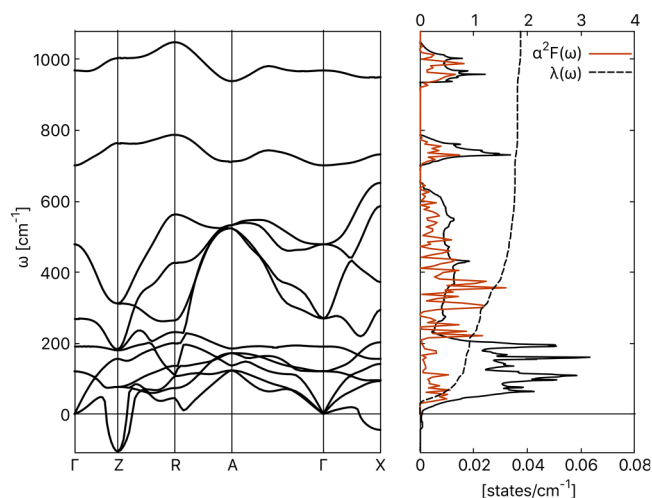


FIG. 7. PdCuH₂ phonon dispersion (right) and relative density of states (left). On the left, we also plot the spectral function (in orange) and its weighted integral $\lambda(\omega)$ (top scale).

making it very promising from a superconducting point of view. Indeed, the $\alpha^2 F(\omega)$ ⁵⁷ function (shown in Fig. 7) is characterized by strongly coupled modes extending up to 500 cm⁻¹, resulting in a total electron–phonon coupling of 1.9 and a $T_C = 40$ –45 K (depending on the parameters used in the numerical evaluation).⁵⁸ The estimation of a larger critical temperature was partially expected, as for PdH, the harmonic approximation yields $T_C = 47$ K⁵³ due to the anomalous softening of phonon frequencies. Anharmonic effects lead to hardening of the phonon spectrum, resulting in a reduction of the critical temperature to 5 K.⁵³

Although the calculation of the anharmonic contributions in PdCuH₂ is beyond the scope of the present paper, we can still estimate the effect of anharmonic corrections on the superconducting properties artificially increasing the phonon frequencies by applying an external pressure. To test this computational experiment, we considered the case of PdH, which is also dynamically unstable at 0 GPa within the harmonic approximation. Increasing the pressure to 15 GPa is enough to reproduce a phonon spectrum in qualitative agreement with the experiments, yielding a critical temperature of 7 K, perfectly in line with what was obtained by means of detailed calculations.⁵³

In the same spirit, we evaluated the phonon frequency at the Z point as a function of the external (isotropic) pressure, finding that it gradually increases and turns real at about 5 GPa, with anharmonic effects strongly reduced (not shown). Thus, to avoid this last critical region, we calculated the phonon spectrum and the electron–phonon coupling of PdCuH₂ at 8 GPa, sufficiently higher than the critical pressure of 5 GPa, but still low enough not to induce relevant changes in electronic properties. The results are reported in Fig. 9, which shows the phonon dispersion and the $\alpha^2 F(\omega)$. We verified that the volume reduction does not have a significant effect neither on electronic properties (the shape of the Fermi surface and the band structure around the Fermi level are

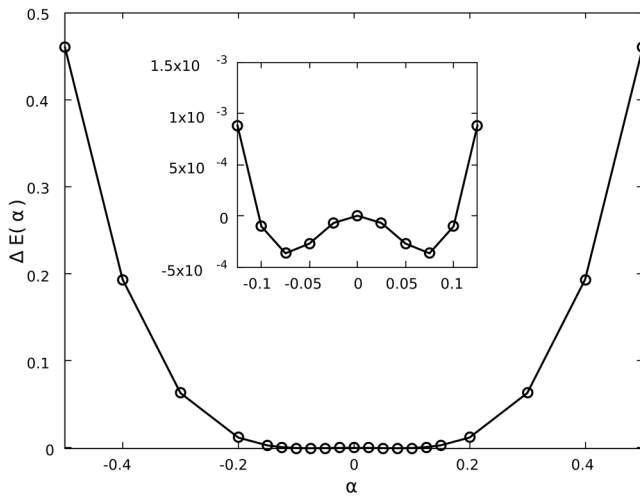


FIG. 8. Adiabatic energy profile (in eV) of PdCuH₂ along the imaginary mode at the Z point. The mode is characterized by eigenvectors with in-plane components on Cu and H atoms in the O2 site. The inset shows a zoom around zero displacement.

practically unchanged with respect to the equilibrium phase) nor on the distribution of the electron–phonon coupling [the $\alpha^2F(\omega)$ spectral function]. However, as expected, the phonon frequencies get shifted to higher energies, in particular, between 200 and 400 cm^{-1} , making the system dynamically stable with real frequencies at both Z- and X-point of the BZ. The electron–phonon coupling is particularly relevant in the intermediate frequency region (400–800 cm^{-1}), characterized by in-plane H vibrations

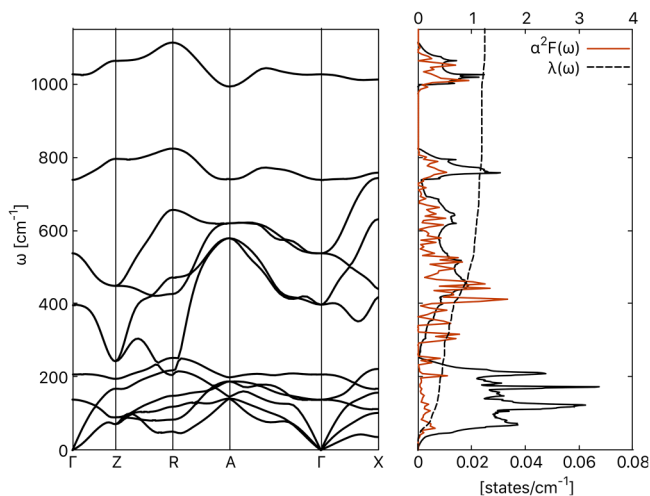


FIG. 9. Phonon dispersion (right) and relative density of states (left) for compressed PdCuH₂ at 8 GPa. On the left, we also plot the spectral function (in orange) and its weighted integral $\lambda(\omega)$ (top scale).

(x/y directions). The higher frequencies originate from the out-of-plane hydrogen modes (z -direction). The predicted total electron–phonon coupling parameter λ is ≈ 1.24 , resulting in a predicted critical temperature of 34 K.

Although this result can quantitatively change due to additional long range distortions and/or anharmonic corrections, we believe that it indicates the possibility of a low, if not ambient, pressure superconducting phase in H-doped PdCu alloys, as obtained in Stritzker’s experiments.³² The hydrogen-rich phase we identified can be a good model to understand the effect of increasing hydrogen content in Pd-alloys, considering that Stritzker’s results were obtained in samples pre-charged under a H₂-gas pressure of 4 atm at 300 °C and subsequently implanted with hydrogen at 130 KV. Indeed, this last result could not be obtained with other techniques, such as high-pressure charging,⁵⁹ but it was possible with electrolytic charging at dry-ice temperatures, one of the most effective techniques to increase hydrogen content in PdH_{*x*} samples.⁶⁰

Interestingly, in PdH, hydrogen doping suppresses spin-fluctuations active in pure Pd,²⁸ which is on the verge of a ferromagnetic phase, favoring the superconducting phase driven by the sizable electron–phonon coupling (already partially present in pure palladium⁸). In contrast, the PdCu alloy does not show any magnetic instabilities, and the electron–phonon coupling is so small ($\lambda \approx 0.2$) that it does not allow a superconducting phase, which is then restored in PdCuH₂ by the presence of hydrogen-derived states at the Fermi level.

IV. CONCLUSIONS

In the present work, using first-principles DFT simulations, we investigated the superconducting properties of PdCuH_{*x*} ternary hydride at ambient pressure ($x = 1, 2$). We were able to rationalize puzzling experimental evidence^{32,60} of a relatively high-temperature superconducting phase in Pd-(noble)-metal alloys, incorporating a significant amount of hydrogen. We identified the low-hydrogen content phase as the PdCuH hydride, predicting the octahedral “O1” site (Fig. 1) as the low energy intercalation site for hydrogen, in good agreement with available experimental data,⁵² but the low electron–phonon coupling parameter excludes this structure as responsible for the observed T_C . On the other hand, the highly hydrogenated structure, i.e., PdCuH₂, possesses interesting superconducting properties, with an estimated T_C of 34 K.

In our opinion, the PdCuH₂ phase, here investigated, can be identified with the one experimentally realized by Stritzker³² and Leiberich *et al.*⁶⁰ The discrepancy in the predicted critical temperature, similarly to what is found for PdH,^{53,61} can be ascribed to anharmonic effects, which, strengthening the phonon frequencies, reduce the critical temperature predicted within the harmonic approximation.

We hope that this work will motivate a careful re-examination of Stritzker’s work, using hydrogen pre-charged samples and hydrogen implantation as an effective technique to increase hydrogen content in Pd–noble-metal alloys, with the goal of engineering new and promising *ambient-pressure* superconducting hydrides.

ACKNOWLEDGMENTS

We wish to acknowledge financial support from the Italian Ministry for Research and Education through PRIN-2017 project “Tuning and understanding quantum phases in 2D materials—Quantum 2D” (IT-MIUR Grant No. 2017Z8TS5B).

AUTHOR DECLARATIONS

Conflict of Interest

All authors declare that they have no conflicts of interest.

DATA AVAILABILITY

The data that support the findings of this study are available from the corresponding authors upon reasonable request.

REFERENCES

- ¹N. W. Ashcroft, “Metallic hydrogen: A high-temperature superconductor?,” *Phys. Rev. Lett.* **21**, 1748–1749 (1968).
- ²R. P. Dias and I. F. Silvera, “Observation of the Wigner-Huntington transition to metallic hydrogen,” *Science* **355**, 715–718 (2017).
- ³P. Loubeyre, F. Occelli, and P. Dumas, “Synchrotron infrared spectroscopic evidence of the probable transition to metal hydrogen,” *Nature* **577**, 631–635 (2020).
- ⁴R. J. Hemley, H. Kwang Mao, A. F. Goncharov, M. Hanfland, and V. Struzhkin, “Synchrotron infrared spectroscopy to 0.15 eV of H₂ and D₂ at megabar pressures,” *Phys. Rev. Lett.* **76**, 1667–1670 (1996).
- ⁵N. H. Chen, E. Sterer, and I. F. Silvera, “Extended infrared studies of high pressure hydrogen,” *Phys. Rev. Lett.* **76**, 1663–1666 (1996).
- ⁶C. Narayana, H. Luo, J. Orloff, and A. L. Ruoff, “Solid hydrogen at 342 GPa: No evidence for an alkali metal,” *Nature* **393**, 46–49 (1998).
- ⁷N. W. Ashcroft, “Hydrogen dominant metallic alloys: High temperature superconductors?,” *Phys. Rev. Lett.* **92**, 187002 (2004).
- ⁸J. A. Flores-Livas, L. Boeri, A. Sanna, G. Profeta, R. Arita, and M. Eremets, “A perspective on conventional high-temperature superconductors at high pressure: Methods and materials,” *Phys. Rep.* **856**, 1–78 (2020).
- ⁹A. P. Drozdov, M. I. Eremets, I. A. Troyan, V. Ksenofontov, and S. I. Shylin, “Conventional superconductivity at 203 kelvin at high pressures in the sulfur hydride system,” *Nature* **525**, 73–76 (2015).
- ¹⁰H. Liu, I. I. Naumov, R. Hoffmann, N. W. Ashcroft, and R. J. Hemley, “Potential high- T_c superconducting lanthanum and yttrium hydrides at high pressure,” *Proc. Natl. Acad. Sci. U.S.A.* **114**, 6990–6995 (2017).
- ¹¹F. Peng, Y. Sun, C. J. Pickard, R. J. Needs, Q. Wu, and Y. Ma, “Hydrogen clathrate structures in rare earth hydrides at high pressures: Possible route to room-temperature superconductivity,” *Phys. Rev. Lett.* **119**, 107001 (2017).
- ¹²M. Somayazulu, M. Ahart, A. K. Mishra, Z. M. Geballe, M. Baldini, Y. Meng, V. V. Struzhkin, and R. J. Hemley, “Evidence for superconductivity above 260 K in lanthanum superhydride at megabar pressures,” *Phys. Rev. Lett.* **122**, 027001 (2019).
- ¹³A. P. Drozdov, P. P. Kong, V. S. Minkov, S. P. Besedin, M. A. Kuzovnikov, S. Mozaffari, L. Balicas, F. F. Balakirev, D. E. Graf, V. B. Prakapenka, E. Greenberg, D. A. Knyazev, M. Tkacz, and M. I. Eremets, “Superconductivity at 250 K in lanthanum hydride under high pressures,” *Nature* **569**, 528–531 (2019).
- ¹⁴E. Snider, N. Dasenbrock-Gammon, R. McBride, X. Wang, N. Meyers, K. V. Lawler, E. Zurek, A. Salamat, and R. P. Dias, “Synthesis of yttrium superhydride superconductor with a transition temperature up to 262 K by catalytic hydrogenation at high pressures,” *Phys. Rev. Lett.* **126**, 117003 (2021).
- ¹⁵L. Boeri, R. G. Hennig, P. J. Hirschfeld, G. Profeta, A. Sanna, E. Zurek, W. E. Pickett, M. Amsler, R. Dias, M. Eremets, C. Heil, R. Hemley, H. Liu, Y. Ma, C. Pierleoni, A. Kolmogorov, N. Rybin, D. Novoselov, V. I. Anisimov, A. R. Oganov, C. J. Pickard, T. Bi, R. Arita, I. Errea, C. Pellegrini, R. Requist, E. Gross, E. R. Margine, S. R. Xie, y. quan, a. hire, L. Fanfarillo, G. R. Stewart, J. J. Hamlin, V. Stanev, R. S. Gonnelli, E. Piatti, D. Romanin, D. Daghero, and R. Valenti, “The 2021 room-temperature superconductivity roadmap,” *J. Phys.: Condens. Matter* (published online 2021).
- ¹⁶E. Snider, N. Dasenbrock-Gammon, R. McBride, M. Debessai, H. Vindana, K. Vencatasamy, K. V. Lawler, A. Salamat, and R. P. Dias, “Room-temperature superconductivity in a carbonaceous sulfur hydride,” *Nature* **586**, 373–377 (2020).
- ¹⁷T. Wang, M. Hirayama, T. Nomoto, T. Koretsune, R. Arita, and J. A. Flores-Livas, “Absence of conventional room temperature superconductivity at high pressure in carbon doped H₃S,” *Phys. Rev. B* **104**, 064510 (2021); [arXiv:2104.03710](https://arxiv.org/abs/2104.03710).
- ¹⁸Z. Zhang, T. Cui, M. J. Hutcheon, A. M. Shipley, H. Song, M. Du, V. Z. Kresin, D. Duan, C. J. Pickard, and Y. Yao, “Design principles for high temperature superconductors with hydrogen-based alloy backbone at moderate pressure,” [arXiv:2106.09879](https://arxiv.org/abs/2106.09879) (2021).
- ¹⁹P. Song, Z. Hou, P. B. de Castro, K. Nakano, K. Hongo, Y. Takano, and R. Maezono, “High-pressure Mg-Sc-H phase diagram and its superconductivity from first-principles calculations,” [arXiv:2109.07051](https://arxiv.org/abs/2109.07051) (2021).
- ²⁰P. Song, Z. Hou, P. B. de Castro, K. Nakano, K. Hongo, Y. Takano, and R. Maezono, “The systematic study on the stability and superconductivity of Y-Mg-H compounds under high pressure,” [arXiv:2107.05498](https://arxiv.org/abs/2107.05498) (2021).
- ²¹S. Di Cataldo, C. Heil, W. von der Linden, and L. Boeri, “LaBH₈: Towards high- T_c low-pressure superconductivity in ternary superhydrides,” *Phys. Rev. B* **104**, L020511 (2021).
- ²²X. Liang, A. Bergara, X. Wei, X. Song, L. Wang, R. Sun, H. Liu, R. J. Hemley, L. Wang, G. Gao, and Y. Tian, “Prediction of high- T_c superconductivity in ternary lanthanum borohydrides,” *Phys. Rev. B* **104**, 134501 (2021).
- ²³M. Gao, X.-W. Yan, Z.-Y. Lu, and T. Xiang, “Phonon-mediated high-temperature superconductivity in the ternary borohydride KB₂H₈ under pressure near 12 GPa,” *Phys. Rev. B* **104**, L100504 (2021).
- ²⁴K. P. Hilleke and E. Zurek, “Tuning chemical precompression: Theoretical design and crystal chemistry of novel hydrides in the quest for warm and light superconductivity at ambient pressures,” [arXiv:2111.03697](https://arxiv.org/abs/2111.03697) (2021).
- ²⁵C. B. Satterthwaite and I. L. Toepke, “Superconductivity of hydrides and deuterides of thorium,” *Phys. Rev. Lett.* **25**, 741–743 (1970).
- ²⁶T. Skoskiewicz, A. W. Szafranski, W. Bujnowski, and B. Baranowski, “Isotope effect in the superconducting palladium-hydrogen-deuterium system,” *J. Phys. C: Solid State Phys.* **7**, 2670–2676 (1974).
- ²⁷B. Stritzker and W. Buckel, “Superconductivity in the palladium-hydrogen and the palladium-deuterium systems,” *Z. Phys. A: Hadrons Nucl.* **257**, 1–8 (1972).
- ²⁸T. Kawae, Y. Inagaki, S. Wen, S. Hirota, D. Itou, and T. Kimura, “Superconductivity in palladium hydride systems,” *J. Phys. Soc. Jpn.* **89**, 051004 (2020).
- ²⁹H. M. Syed, T. J. Gould, C. J. Webb, and E. M. Gray, “Superconductivity in palladium hydride and deuteride at 52–61 kelvin,” [arXiv:1608.01774](https://arxiv.org/abs/1608.01774) (2016).
- ³⁰P.-W. Guan, R. J. Hemley, and V. Viswanathan, “Combining pressure and electrochemistry to synthesize superhydrides,” *Proc. Natl. Acad. Sci. U.S.A.* **118**, e2110470118 (2021).
- ³¹Z. M. Geballe, M. Somayazulu, N. Armanet, A. K. Mishra, M. Ahart, and R. J. Hemley, “High-pressure synthesis and thermodynamic stability of PdH_{1+ε} up to 8 GPa,” *Phys. Rev. B* **103**, 024515 (2021).
- ³²B. Stritzker, “High superconducting transition temperatures in the palladium-noble metal-hydrogen system,” *Z. Phys.* **268**, 261–264 (1974).
- ³³P. Giannozzi, S. Baroni, N. Bonini, M. Calandra, R. Car, C. Cavazzoni, D. Ceresoli, G. L. Chiarotti, M. Cococcioni, I. Dabo, A. D. Corso, S. de Gironcoli, S. Fabris, G. Fratesi, R. Gebauer, U. Gerstmann, C. Gougousis, A. Kokalj, M. Lazzeri, L. Martin-Samos, N. Marzari, F. Mauri, R. Mazzarello, S. Paolini, A. Pasquarello, L. Paulatto, C. Sbraccia, S. Scandolo, G. Sclauzero, A. P. Seitsonen, A. Smogunov, P. Umari, and R. M. Wentzcovitch, “QUANTUM ESPRESSO: A modular and open-source software project for quantum simulations of materials,” *J. Phys.: Condens. Matter* **21**, 395502 (2009).

- ³⁴P. Giannozzi, O. Andreussi, T. Brumme, O. Bunau, M. B. Nardelli, M. Calandra, R. Car, C. Cavazzoni, D. Ceresoli, M. Cococcioni, N. Colonna, I. Carnimeo, A. D. Corso, S. de Gironcoli, P. Delugas, R. A. DiStasio, A. Ferretti, A. Floris, G. Fratesi, G. Fugallo, R. Gebauer, U. Gerstmann, F. Giustino, T. Gorni, J. Jia, M. Kawamura, H.-Y. Ko, A. Kokalj, E. Küçükbenli, M. Lazzeri, M. Marsili, N. Marzari, F. Mauri, N. L. Nguyen, H.-V. Nguyen, A. O. de-la Roza, L. Paulatto, S. Poncé, D. Rocca, R. Sabatini, B. Santra, M. Schlipf, A. P. Seitsonen, A. Smogunov, I. Timrov, T. Thonhauser, P. Umari, N. Vast, X. Wu, and S. Baroni, “Advanced capabilities for materials modelling with Quantum ESPRESSO,” *J. Phys.: Condens. Matter* **29**, 465901 (2017).
- ³⁵W. Kohn and L. J. Sham, “Self-consistent equations including exchange and correlation effects,” *Phys. Rev.* **140**, A1133–A1138 (1965).
- ³⁶D. Vanderbilt, “Soft self-consistent pseudopotentials in a generalized eigenvalue formalism,” *Phys. Rev. B* **41**, 7892–7895 (1990).
- ³⁷D. R. Hamann, “Erratum: Optimized norm-conserving Vanderbilt pseudopotentials [Phys. Rev. B **88**, 085117 (2013)],” *Phys. Rev. B* **95**, 239906 (2017).
- ³⁸X. Gonze, “Perturbation expansion of variational principles at arbitrary order,” *Phys. Rev. A* **52**, 1086–1095 (1995).
- ³⁹Also, the k -mesh for self-consistent calculation was raised to $21 \times 21 \times 21$ to better converge the derivative of the total energy.
- ⁴⁰P. B. Allen and R. C. Dynes, “Transition temperature of strong-coupled superconductors reanalyzed,” *Phys. Rev. B* **12**, 905–922 (1975).
- ⁴¹A. Kokalj, “XCrySDen—A new program for displaying crystalline structures and electron densities,” *J. Mol. Graph. Model.* **17**, 176–179 (1999).
- ⁴²K. Zhang and J. D. Way, “Palladium-copper membranes for hydrogen separation,” *Sep. Purif. Technol.* **186**, 39–44 (2017).
- ⁴³Y. Hu and H. Gong, “First principles study of thermodynamic and mechanical properties of Pd₅₀Cu₅₀,” *J. Alloys Compd.* **639**, 635–641 (2015).
- ⁴⁴S. Nayebossadri, J. Speight, and D. Book, “Effects of low Ag additions on the hydrogen permeability of Pd–Cu–Ag hydrogen separation membranes,” *J. Memb. Sci.* **451**, 216–225 (2014).
- ⁴⁵P. Huang, S. Menon, and D. de Fontaine, “On the Cu–Pd phase diagram,” *J. Phase Equilib.* **12**, 3–5 (1991).
- ⁴⁶V. E. Antonov, I. T. Belash, E. G. Ponyatovskii, and V. I. Rashupkin, “Superconductivity of solid hydrogen solutions in palladium alloys with noble metals,” *JETP Lett.* **31**, 451 (1980).
- ⁴⁷H. Li, Z. Dong, F. Yang, and W. Ruilan, “Effect of ion beam mixing/implantation at low temperature on superconductivity in palladium-hydrogen and palladium-copper-hydrogen systems,” *Chin. Phys. Lett.* **4**, 241–244 (1987).
- ⁴⁸A. Irodova, V. Glazkov, V. Somenkov, V. Antonov, and E. Ponyatovsky, “Hydrogen caused ordering in PdAg alloys,” *Z. Phys. Chem.* **163**, 53–57 (1989).
- ⁴⁹E. Bruno and B. Ginatempo, “On the fcc-B₂ transformation in CuPd alloys,” *Europhys. Lett.* **42**, 649–654 (1998).
- ⁵⁰P. Subramanian and D. Laughlin, “Cu–Pd (copper–palladium),” *J. Phase Equilib.* **12**, 231–243 (1991).
- ⁵¹G. Bozzolo, J. E. Garcés, R. D. Noebe, P. Abel, and H. O. Mosca, “Atomistic modeling of surface and bulk properties of Cu, Pd and the Cu–Pd system,” *Prog. Surf. Sci.* **73**, 79–116 (2003).
- ⁵²A. I. Kolesnikov, V. E. Antonov, A. M. Balagurov, S. Bennington, and M. Prager, “Neutron scattering studies of the structure and dynamics of the PdCu–H ordered phase produced under a high hydrogen pressure,” *J. Phys.: Condens. Matter* **6**, 9001–9008 (1994).
- ⁵³I. Errea, M. Calandra, and F. Mauri, “First-principles theory of anharmonicity and the inverse isotope effect in superconducting palladium-hydride compounds,” *Phys. Rev. Lett.* **111**, 177002 (2013).
- ⁵⁴M. P. Belov, A. B. Syzdykova, Y. K. Vekilov, and I. A. Abrikosov, “Hydrogen in palladium: Anharmonicity of lattice dynamics from first principles,” *Phys. Solid State* **57**, 260–265 (2015).
- ⁵⁵We ignore the contribution of unstable phonon modes at the R point (which will produce a superstructure) to the electron–phonon coupling.
- ⁵⁶In order to avoid overestimation of λ due to the dynamical instability, we discarded all the contributions of frequencies below 20 cm^{-1} .
- ⁵⁷As for PdCuH, we discard frequencies below 20 cm^{-1} .
- ⁵⁸Since $\lambda > 1.5$, the modified Allen and Dynes⁴⁰ equation was used.
- ⁵⁹T. Skośkiewicz, A. W. Szafranski, and B. Baranowski, “Superconductivity of some palladium alloys hydrogenized at high pressure conditions,” *Phys. Status Solidi B* **59**, K135–K136 (1973).
- ⁶⁰A. Leiberich, W. Scholz, W. Standish, and C. Homan, “Superconductivity in H-charged Cu-implanted Pd,” *Phys. Lett. A* **87**, 57–60 (1981).
- ⁶¹A. E. Karakozov and E. G. Maksimov, “Influence of anharmonicity on superconductivity,” *Sov. Phys.—JETP* **47**, 681 (1978).